



Search for CP violation in $\Lambda_b^0 \rightarrow pK^-$ and $\Lambda_b^0 \rightarrow p\pi^-$ decays

LHCb Collaboration



ARTICLE INFO

Article history:

Received 18 July 2018

Received in revised form 21 September 2018

Accepted 19 October 2018

Available online 24 October 2018

Editor: L. Rolandi

ABSTRACT

A search for CP violation in $\Lambda_b^0 \rightarrow pK^-$ and $\Lambda_b^0 \rightarrow p\pi^-$ decays is presented using a sample of pp collisions collected with the LHCb detector and corresponding to an integrated luminosity of 3.0 fb^{-1} . The CP -violating asymmetries are measured to be $A_{CP}^{pK^-} = -0.020 \pm 0.013 \pm 0.019$ and $A_{CP}^{p\pi^-} = -0.035 \pm 0.017 \pm 0.020$, and their difference $A_{CP}^{pK^-} - A_{CP}^{p\pi^-} = 0.014 \pm 0.022 \pm 0.010$, where the first uncertainties are statistical and the second systematic. These are the most precise measurements of such asymmetries to date.

© 2018 The Author(s). Published by Elsevier B.V. This is an open access article under the CC BY license (<http://creativecommons.org/licenses/by/4.0/>). Funded by SCOAP³.

1. Introduction

The non-invariance of weak interactions under the combined application of charge conjugation (C) and parity (P) transformations is accommodated within the Standard Model by the Cabibbo-Kobayashi-Maskawa mechanism [1,2]. The violation of the CP symmetry was discovered in neutral-kaon decays [3], and later observed with B^0 [4–12], B^+ [13] and B_s^0 mesons [12,14]. First evidence for CP violation in the b -baryon sector was found more recently [15]. The decays $\Lambda_b^0 \rightarrow pK^-$ and $\Lambda_b^0 \rightarrow p\pi^-$ are mediated by the same quark-level transitions contributing to charmless two-body B^0 and B_s^0 decays to charged pions and kaons, where nonzero values of the CP asymmetries are well established [14]. The inclusion of charge-conjugate processes is implied throughout.

Predictions for the CP asymmetries in the decays of the Λ_b^0 baryon to two-body charmless final states pK^- or $p\pi^-$ range from a few percent in the generalised factorisation approach [16, 17] up to approximately 30% within the perturbative quantum-chromodynamics formalism [18]. The only measurements of these quantities available to date were performed by the CDF Collaboration [12]. The asymmetries were found to be compatible with zero within an uncertainty of 8 to 9%.

This Letter reports on a search for CP violation in $\Lambda_b^0 \rightarrow pK^-$ and $\Lambda_b^0 \rightarrow p\pi^-$ decays, using pp -collision data collected with the LHCb detector at centre-of-mass energies of 7 and 8 TeV and corresponding to 3.0 fb^{-1} of integrated luminosity. The CP asymmetry is defined as

$$A_{CP}^f \equiv \frac{\Gamma(\Lambda_b^0 \rightarrow f) - \Gamma(\bar{\Lambda}_b^0 \rightarrow \bar{f})}{\Gamma(\Lambda_b^0 \rightarrow f) + \Gamma(\bar{\Lambda}_b^0 \rightarrow \bar{f})}, \quad (1)$$

where Γ is the partial width of the given decay, with $f \equiv pK^-$ ($p\pi^-$) and $\bar{f} \equiv \bar{p}K^+$ ($\bar{p}\pi^+$). In addition, the difference of

the two CP asymmetries, $\Delta A_{CP} \equiv A_{CP}^{pK^-} - A_{CP}^{p\pi^-}$, is also reported. As the main systematic uncertainties cancel in the difference, this quantity will become useful with the increasing size of the data sample.

The Letter is organised as follows. After a brief introduction on the detector, trigger and simulation in Sec. 2, the formalism needed to relate the physical CP asymmetries to the experimental measurements is presented in Sec. 3. Then, the event selection and the invariant-mass fit are described in Secs. 4 and 5, respectively. The determination of instrumental asymmetries and systematic uncertainties is discussed in Sec. 6. Finally, results are given and conclusions are drawn in Sec. 7.

2. Detector, trigger and simulation

The LHCb detector [19,20] is a single-arm forward spectrometer covering the pseudorapidity range $2 < \eta < 5$, designed for the study of particles containing b or c quarks. The detector includes a high-precision tracking system consisting of a silicon-strip vertex detector surrounding the pp interaction region [21], a large-area silicon-strip detector located upstream of a dipole magnet with a bending power of about 4 Tm, and three stations of silicon-strip detectors and straw drift tubes [22] placed downstream of the magnet. The tracking system provides a measurement of the momentum, p , of charged particles with a relative uncertainty that varies from 0.5% at low momentum to 1.0% at $200\text{ GeV}/c$. The minimum distance of a track to a primary vertex (PV), the impact parameter (IP), is measured with a resolution of $(15 + 29/p_T)\mu\text{m}$, where p_T is the component of the momentum transverse to the beam, in GeV/c . Different types of charged hadrons are distinguished using information from two ring-imaging Cherenkov detectors [23]. Photons, electrons and hadrons are identified by a calorimeter system consisting of scintillating-pad and preshower

detectors, an electromagnetic calorimeter and a hadronic calorimeter. Muons are identified by a system composed of alternating layers of iron and multiwire proportional chambers [24]. The online event selection is performed by a trigger [25], which consists of a hardware stage, based on information from the calorimeter and muon systems, followed by a software stage, which applies a full event reconstruction.

Simulated events are used to study the modelling of various mass line shapes. In the simulation, proton–proton collisions are generated using PYTHIA [26] with a specific LHCb configuration [27]. Decays of hadronic particles are described by EvtGen [28], in which final-state radiation is generated using PHOTOS [29]. The interaction of the generated particles with the detector and its response are implemented using the GEANT4 toolkit [30] as described in Ref. [31].

3. Formalism

The CP asymmetries of $\Lambda_b^0 \rightarrow pK^-$ and $\Lambda_b^0 \rightarrow p\pi^-$ decays are approximated as the sums of various experimental quantities

$$A_{CP}^{pK^-} = A_{\text{raw}}^{pK^-} - A_D^p - A_D^{K^-} - A_{\text{PID}}^{pK^-} - A_p^{\Lambda_b^0} - A_{\text{trigger}}^{pK^-}, \quad (2)$$

$$A_{CP}^{p\pi^-} = A_{\text{raw}}^{p\pi^-} - A_D^p - A_D^{\pi^-} - A_{\text{PID}}^{p\pi^-} - A_p^{\Lambda_b^0} - A_{\text{trigger}}^{p\pi^-}, \quad (3)$$

where A_{raw}^f is the measured raw asymmetry between the yields of the decays $\Lambda_b^0 \rightarrow f$ and $\bar{\Lambda}_b^0 \rightarrow \bar{f}$, with $f = pK^-$ ($p\pi^-$) and \bar{f} its charge conjugate; A_D^h is the asymmetry between the detection efficiencies for particle h and its charge conjugate, with $h = p$, K^- or π^- ; the symbol A_{PID}^f stands for the asymmetry between the particle-identification (PID) efficiencies for the final states f and \bar{f} ; $A_p^{\Lambda_b^0}$ is the asymmetry between the production cross-sections of Λ_b^0 and $\bar{\Lambda}_b^0$ baryons; and A_{trigger}^f is the asymmetry between the trigger efficiencies for the particles in the final states f and \bar{f} . This linear approximation is valid to a good enough accuracy due to the smallness of the terms involved.

The raw asymmetry is defined as

$$A_{\text{raw}}^f \equiv \frac{N(\Lambda_b^0 \rightarrow f) - N(\bar{\Lambda}_b^0 \rightarrow \bar{f})}{N(\Lambda_b^0 \rightarrow f) + N(\bar{\Lambda}_b^0 \rightarrow \bar{f})}, \quad (4)$$

where N denotes the observed signal yield for the given decay, obtained in this analysis by means of extended binned maximum-likelihood fits to the pK^- and $p\pi^-$ invariant-mass spectra.

The proton, kaon and pion detection asymmetries are defined as

$$A_D^p \equiv \frac{\varepsilon_{\text{rec}}^p - \varepsilon_{\text{rec}}^{\bar{p}}}{\varepsilon_{\text{rec}}^p + \varepsilon_{\text{rec}}^{\bar{p}}}, \quad A_D^{K^-} \equiv \frac{\varepsilon_{\text{rec}}^{K^-} - \varepsilon_{\text{rec}}^{K^+}}{\varepsilon_{\text{rec}}^{K^-} + \varepsilon_{\text{rec}}^{K^+}}, \quad A_D^{\pi^-} \equiv \frac{\varepsilon_{\text{rec}}^{\pi^-} - \varepsilon_{\text{rec}}^{\pi^+}}{\varepsilon_{\text{rec}}^{\pi^-} + \varepsilon_{\text{rec}}^{\pi^+}}, \quad (5)$$

where ε_{rec} is the total efficiency to reconstruct the given particle, excluding PID. Such asymmetries are mostly due to the different interaction cross-sections of particles and antiparticles with the detector material. The kaon and pion detection asymmetries are measured using charm-meson control samples employing the procedures described in Refs. [32,33]. The kaon detection asymmetry is obtained by subtracting the raw asymmetries of the $D^+ \rightarrow K_S^0 \pi^+$ and $D^+ \rightarrow K^-\pi^+\pi^+$ decay modes and correcting for the K^0 ($A_D^{K^0}$) [32] and pion detection asymmetries. The latter is measured from the ratio of partially to fully reconstructed $D^{*+} \rightarrow D^0 (\rightarrow K^-\pi^+\pi^+\pi^-)\pi^+$ decays. The proton detection asymmetry is obtained from simulated events.

The PID asymmetries are measured from large calibration samples and are defined as

$$A_{\text{PID}}^f \equiv \frac{\varepsilon_{\text{PID}}^f - \varepsilon_{\text{PID}}^{\bar{f}}}{\varepsilon_{\text{PID}}^f + \varepsilon_{\text{PID}}^{\bar{f}}}, \quad (6)$$

where $\varepsilon_{\text{PID}}^{f(\bar{f})}$ is the PID efficiency for a final state $f(\bar{f})$ given a set of PID requirements.

The Λ_b^0 production asymmetry is defined as

$$A_P^{\Lambda_b^0} = \frac{\sigma(\Lambda_b^0) - \sigma(\bar{\Lambda}_b^0)}{\sigma(\Lambda_b^0) + \sigma(\bar{\Lambda}_b^0)}, \quad (7)$$

where σ denotes the inclusive production cross-section in the LHCb acceptance. The production asymmetry is taken as an external input, following Ref. [34].

Finally, asymmetries may arise if the hardware and software trigger used to collect data do not have the same efficiencies on oppositely charged particles. These effects are estimated through various data-driven techniques, as described in Sec. 6.

4. Event selection

The event selection starts with the reconstruction of b hadrons formed by two oppositely charged tracks with $p_T > 1 \text{ GeV}/c$, inconsistent with originating from any PV and required to form a common vertex. Each b -hadron candidate needs to have a transverse momentum greater than $1.2 \text{ GeV}/c$ and an invariant mass, computed assigning the pion mass to both daughter tracks, in the range between 4.8 and $5.8 \text{ GeV}/c^2$. Finally, each b -hadron candidate is required to be consistent with originating from a PV.

Particle-identification selection criteria are applied to divide the data sample into mutually exclusive subsamples corresponding to the final-state hypotheses pK^- , $\bar{p}K^+$, $p\pi^-$, $\bar{p}\pi^+$, $K^+\pi^-$, $K^-\pi^+$, K^+K^- and $\pi^+\pi^-$. The latter four combinations are selected to study the background due to two-body B decays, where one or both final-state particles are misidentified.

The event selection is further refined using a boosted decision tree (BDT) classifier [35,36] to reject combinatorial background. This algorithm combines the information from several input quantities to obtain a discriminant variable used to classify the b -hadron candidates as signal or background. The following properties of the final-state particles are used as input variables: the transverse momentum of the b -hadron decay products, the logarithms of their χ_{IP}^2 values, where χ_{IP}^2 is defined as the difference in the vertex-fit χ^2 of a given PV reconstructed with and without the candidate under consideration, the quality of the common vertex fit of the two tracks and the distance of closest approach between the two tracks. The BDT also exploits the following properties of the b -hadron candidate: the transverse momentum, the χ_{IP}^2 quantity, and the logarithm of the flight distance with respect to the associated PV, defined as that with the smallest χ_{IP}^2 with respect to the b -hadron candidate. The BDT is trained using simulated signal decays and combinatorial background events from data in the high-mass sideband.

The selection criteria on the BDT classifier and the PID variables are optimised separately for the $\Lambda_b^0 \rightarrow pK^-$ and $\Lambda_b^0 \rightarrow p\pi^-$ decays. Two different selections, denoted hereafter as S_{pK^-} and $S_{p\pi^-}$, are aimed at obtaining the best statistical sensitivity on each of the two CP asymmetries. Common PID requirements are used for the final states containing only kaons and pions. Multiple candidates are present in less than 0.05% of the events in the final sample. Only one candidate is accepted for each event on the basis of a reproducible pseudorandom sequence.

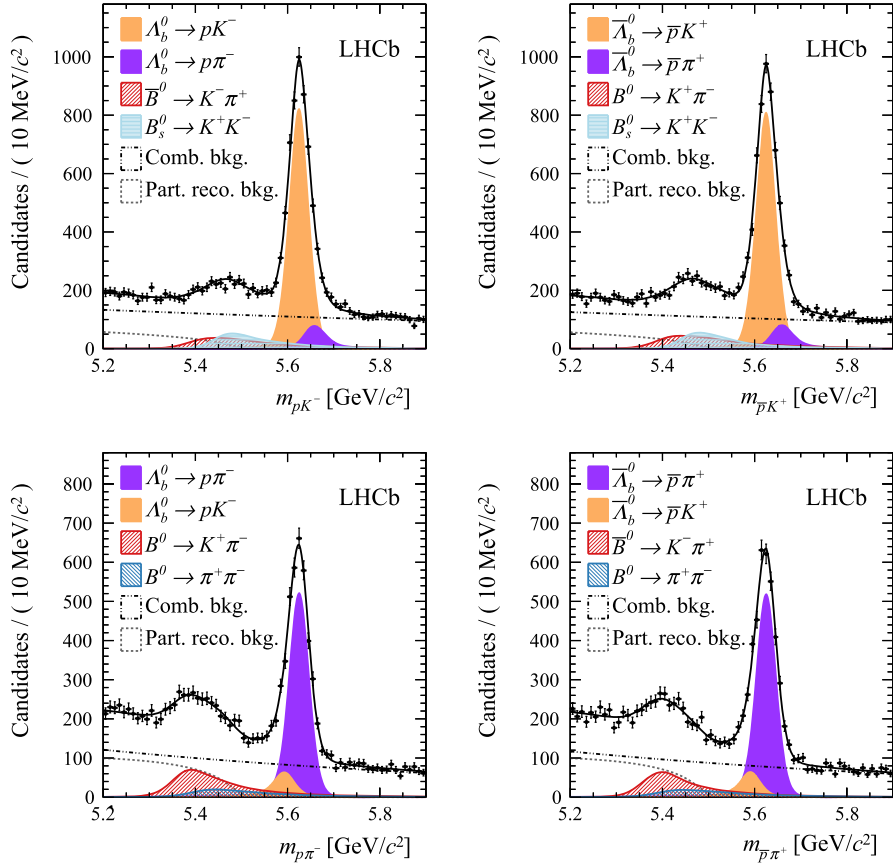


Fig. 1. Invariant-mass distributions: (top left) m_{pK^-} , (top right) $m_{\bar{p}K^+}$, (bottom left) $m_{p\pi^-}$ and (bottom right) $m_{\bar{p}\pi^+}$ for candidates passing the (top) S_{pK^-} and (bottom) $S_{p\pi^-}$ selections. The results of the fits are superimposed.

5. Invariant-mass fit

For each final-state hypothesis, namely pK^- , $\bar{p}K^+$, $p\pi^-$, $\bar{p}\pi^+$, $K^+\pi^-$, $K^-\pi^+$, K^+K^- and $\pi^+\pi^-$, the invariant-mass distribution of selected candidates is modelled by an appropriate probability density function. These models are used to perform a simultaneous fit to the eight invariant-mass spectra and determine at once the yields of all two-body b -hadron decays contributing to the spectra. Three categories are considered for the background: combinatorial, due to random association of tracks; partially reconstructed, due to multibody b -hadron decays with one or more particles not reconstructed; and cross-feed, arising from other two-body b -hadron decays where one or both final-state particles are misidentified.

The model used to describe each signal is obtained by convolving the sum of two Gaussian functions with common mean, accounting for mass-resolution effects, with a power-law function that accounts for final-state photon radiation effects. The power-law distribution is taken from analytical quantum-electrodynamics calculations [37] and the correctness of the model is checked against simulated events generated with PHOTOS [29]. The parameter governing the tail due to final-state photon radiation effects is different for each decay mode. This model describes well the invariant-mass distributions predicted by the simulation.

The combinatorial background is modelled using exponential functions. The partially reconstructed background is parameterised using ARGUS functions [38] convolved with the sum of two Gaussian functions with zero mean values, whose relative fraction and widths are in common with the signal model. Finally, the cross-feed background is modelled using simulated two-body b -hadron decays and a kernel estimation method [39]. The cross-feed back-

ground yields are set to the corresponding two-body b -hadron decay yields, determined by the simultaneous fit, multiplied by appropriate PID efficiency ratios. The efficiencies for a given PID requirement are obtained from large calibration samples of $D^{*+} \rightarrow D^0(\rightarrow K^-\pi^+)\pi^+$, $\Lambda \rightarrow p\pi^-$ and $\Lambda_c^+ \rightarrow pK^-\pi^+$ decays, with the aid of simulated events in the case of protons to account for phase-space regions not covered by the calibration samples (about 20% of the protons from signal decays). The efficiencies are determined in bins of particle momentum, pseudorapidity and track multiplicity, as the performances of the RICH detectors depend on such variables. They are then averaged over the momentum and pseudorapidity distributions of the final-state particles and over the distribution of track multiplicity in selected events.

After the application of the optimal BDT and PID requirements, an extended binned maximum-likelihood fit with a bin width of $5 \text{ MeV}/c^2$ is performed simultaneously to the eight two-body invariant-mass spectra for each of the two selections, S_{pK^-} and $S_{p\pi^-}$. The m_{pK^-} and $m_{p\pi^-}$ invariant-mass distributions are shown in Fig. 1, with the results of the fits superimposed. The values of the raw asymmetries and of the signal yields obtained from the fits to the candidates passing the respective S_{pK^-} or $S_{p\pi^-}$ selection are $A_{\text{raw}}^{pK^-} = (1.0 \pm 1.3)\%$, $A_{\text{raw}}^{p\pi^-} = (0.5 \pm 1.7)\%$, $N_{\text{sig}}^{pK^-} + N_{\text{sig}}^{\bar{p}K^+} = 8847 \pm 125$ and $N_{\text{sig}}^{p\pi^-} + N_{\text{sig}}^{\bar{p}\pi^+} = 6026 \pm 105$.

The fit is validated by generating a large number of pseudo-experimental data samples according to the total probability density function of the model and performing an extended binned maximum-likelihood fit to each sample. The resulting pull distributions for $A_{\text{raw}}^{pK^-}$ and $A_{\text{raw}}^{p\pi^-}$ are found to be Gaussian with zero means and unitary widths.

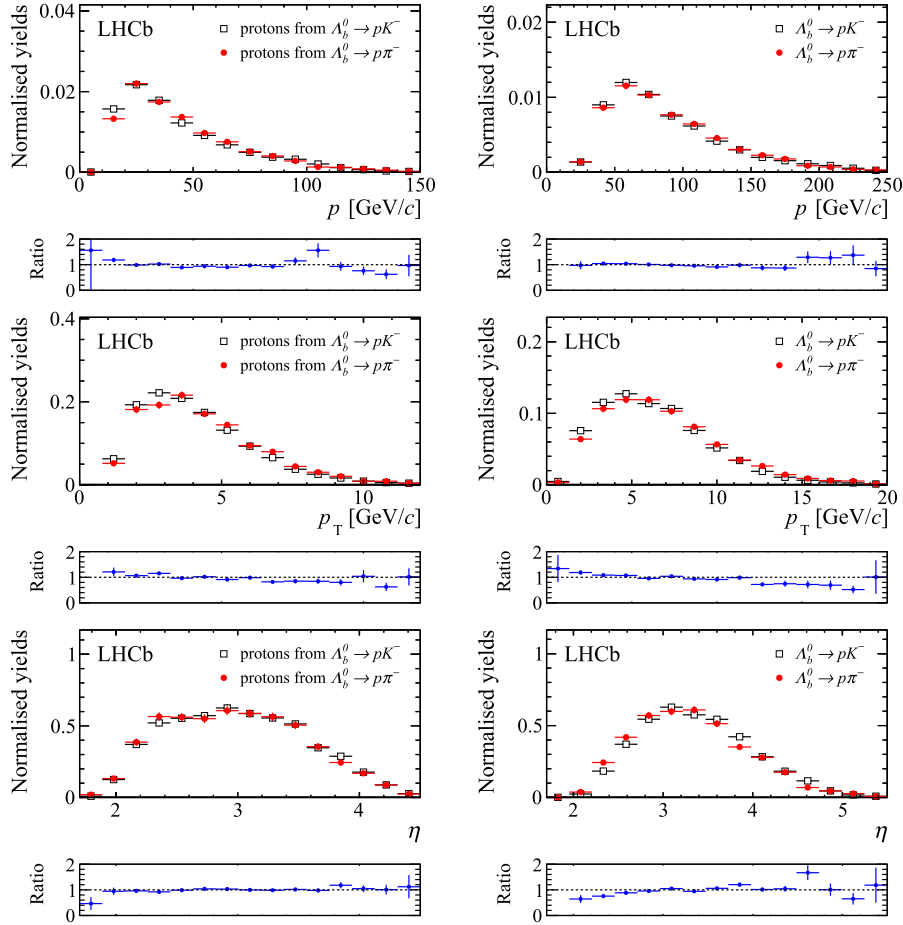


Fig. 2. Distributions of (top) momentum, (middle) transverse momentum and (bottom) pseudorapidity for (left) protons from Λ_b^0 decays and (right) Λ_b^0 baryons. The distributions are background-subtracted and normalised to unit area. Below each plot the ratio between the two distributions corresponding to $\Lambda_b^0 \rightarrow pK^-$ and $\Lambda_b^0 \rightarrow p\pi^-$ decays is also shown.

6. Instrumental asymmetries and systematic uncertainties

The determination of the instrumental asymmetries introduced in Eqs. (2) and (3) is crucial to obtain the CP asymmetries, as described in Sec. 3.

The kaon detection asymmetry is determined as a function of the kaon momentum, following the approach developed in Ref. [32] and subtracting $A_D^{K^0} = (0.054 \pm 0.014)\%$ [32] and the pion detection asymmetry. The momentum-dependent values are then weighted with the background-subtracted [40] momentum distribution of kaons from $\Lambda_b^0 \rightarrow pK^-$ decays to obtain $A_D^{K^-} = (-0.76 \pm 0.23)\%$, where the dominant uncertainty is due to the finite size of the samples used. The pion detection asymmetry is obtained in an analogous way, adopting the approach of Ref. [33], and is determined to be $A_D^{\pi^-} = (0.13 \pm 0.11)\%$. A different approach is followed for the proton detection asymmetry, since no measurement of this quantity is available to date. Simulated events are used to obtain the reconstruction efficiency defined as the number of reconstructed over generated decays, in bins of proton momentum. Then, according to Eq. (5), an asymmetry is defined and weights are computed from the background-subtracted [40] proton-momentum distributions of $\Lambda_b^0 \rightarrow pK^-$ and $\Lambda_b^0 \rightarrow p\pi^-$ decays. The proton detection asymmetries for both decays are found to be equal, consistent with the fact that the kinematics of the protons for the two decays do not exhibit significant differences, as shown in Fig. 2. The common value is $A_D^p = (1.30 \pm 0.03 \pm 0.16 \pm 0.65)\%$, where the first uncertainty is due to the finite amount of

simulated events and the second is associated to the knowledge of the material budget of the LHCb detector. The third uncertainty is due to the assumptions made on the proton and antiproton cross-sections used in the computation.

The PID asymmetries are calculated using calibration samples with the aid of simulation to account for the limited phase-space coverage of the protons from $\Lambda \rightarrow p\pi^-$ and $\Lambda_c^+ \rightarrow pK^-\pi^+$ decays. The dominant uncertainty comes from different PID performances in data and simulation in the phase-space region where simulated events are used. This discrepancy has been studied using $B^0 \rightarrow K^+\pi^-$ decays, for which the phase-space coverage of calibration data is larger. The values of the PID asymmetries are found to be $A_{\text{PID}}^{pK^-} = (-0.30 \pm 0.74)\%$ and $A_{\text{PID}}^{p\pi^-} = (-0.18 \pm 0.73)\%$.

The integrated Λ_b^0 production asymmetries are calculated convolving the background-subtracted [40] two-dimensional transverse-momentum and rapidity distributions of $\Lambda_b^0 \rightarrow pK^-$ and $\Lambda_b^0 \rightarrow p\pi^-$ candidates with the production asymmetries measured as a function of the same variables reported in Ref. [34]. Since Λ_b^0 baryons selected in the pK^- or $p\pi^-$ final states have very similar kinematics, as shown in Fig. 2, the value $A_p^{\Lambda_b^0} = (2.7 \pm 1.4)\%$, averaged for 7 and 8 TeV data, is obtained for the production asymmetry of both decays.

Asymmetries related to different trigger efficiencies for the charge-conjugated final states may arise. The efficiency for a charged hadron to be responsible for the affirmative decision of the hardware trigger is determined as a function of transverse

Table 1Systematic uncertainties on $A_{CP}^{pK^-}$ and $A_{CP}^{p\pi^-}$.

Systematic uncertainty	$A_{CP}^{pK^-}$ [%]	$A_{CP}^{p\pi^-}$ [%]
Kaon or pion detection asymmetry	0.23	0.11
Proton detection asymmetry	0.67	0.67
PID asymmetry	0.74	0.73
Λ_b^0 production asymmetry	1.40	1.40
Trigger asymmetry	0.53	0.55
Signal model	0.02	0.02
Background model	0.23	0.47
PID efficiencies	0.57	0.74
Total	1.91	2.00

momentum, separately for positively and negatively charged particles, using a sample of $\Lambda_b^0 \rightarrow \Lambda_c^+ (\rightarrow pK^-\pi^+)\pi^-$ decays. These efficiencies are used to determine the charge asymmetry introduced by the hardware trigger for the signal candidates that fire it. The charge asymmetry introduced by the hardware trigger for candidates that are retained independently of whether or not they are responsible for an affirmative hardware-trigger decision is determined studying a sample of $B^0 \rightarrow K^+\pi^-$ decays [25]. The asymmetry of the software trigger is also studied using $B^0 \rightarrow K^+\pi^-$ decays, determining the charge asymmetry of the fraction of $B^0 \rightarrow K^+\pi^-$ decays for which both final-state hadrons fire the software trigger with respect to those for which only one hadron fires. The total trigger asymmetries are measured to be $A_{\text{trigger}}^{pK^-} = (0.18 \pm 0.53)\%$ and $A_{\text{trigger}}^{p\pi^-} = (-0.08 \pm 0.55)\%$. The uncertainties are mainly due to the limited size of the samples used in their determination.

Several sources of systematic uncertainties associated with the fit model are investigated. The alternative models used to determine systematic uncertainties associated with the choices of the invariant-mass shapes consist in turn of: adding a Gaussian function to the invariant-mass resolution model used for signals and cross-feed backgrounds to account for long tails due to candidates with a poor determination of the final-state particles momenta; changing the value of the parameter governing the final-state photon radiation effects according to its uncertainty; substituting the exponential function used to model the combinatorial background with a linear function and removing the partially reconstructed background component by rejecting candidates with m_{K^-} ($m_{p\pi^-}$) lower than $5.5 \text{ GeV}/c^2$. When testing alternative models, 250 pseudoexperiments are generated according to the baseline fit model and using as input the central values of the baseline results. Fits are performed to each of the generated samples using the baseline model and then the alternative models. The mean and the root mean square of the distribution of the difference between the raw asymmetries determined by the two sets of fits are added in quadrature and the resulting value is taken as a systematic uncertainty.

A different approach is adopted to assess systematic uncertainties related to the knowledge of the PID efficiencies. Samples are generated using the baseline fit model and results. The baseline fit model is then fitted 250 times to the generated samples, varying the PID efficiencies according to their uncertainties, which are mainly driven by the choice of the binning scheme used to divide the phase-space. These uncertainties are assessed by changing the baseline binning scheme with alternative schemes and computing again the efficiencies. The largest root mean square of the raw asymmetry distributions is taken as a systematic uncertainty.

The systematic uncertainties due to the fit model choice, PID efficiencies determination and instrumental asymmetries measurement, along with the total uncertainty obtained as the quadratic sum of the individual contributions, are reported in Table 1.

7. Results and conclusions

Using in Eqs. (2) and (3) the values of the raw asymmetries reported in Sec. 5 and those of the instrumental and production asymmetries reported in Sec. 6, the following CP asymmetries are obtained

$$A_{CP}^{pK^-} = -0.020 \pm 0.013 \pm 0.019,$$

$$A_{CP}^{p\pi^-} = -0.035 \pm 0.017 \pm 0.020,$$

where the first uncertainties are statistical and the second systematic. The correlation between $A_{CP}^{pK^-}$ and $A_{CP}^{p\pi^-}$ is found to be 0.5. No evidence for CP violation is observed.

A quantity that is independent from the proton detection and Λ_b^0 production asymmetries is obtained by taking the difference

$$\Delta A_{CP} \equiv A_{CP}^{pK^-} - A_{CP}^{p\pi^-} = A_{\text{raw}}^{pK^-} - A_{D}^{K^-} - A_{\text{PID}}^{pK^-} - A_{\text{trigger}}^{pK^-} - A_{\text{raw}}^{p\pi^-} + A_{D}^{\pi^-} + A_{\text{PID}}^{p\pi^-} + A_{\text{trigger}}^{p\pi^-}. \quad (8)$$

The statistical and systematic correlations between the raw asymmetries, the PID asymmetries and the detection asymmetries are taken into account when propagating the uncertainty to ΔA_{CP} , obtaining

$$\Delta A_{CP} = 0.014 \pm 0.022 \pm 0.010,$$

where the first uncertainty is statistical and the second systematic. These results represent the world's best measurements to date, with much improved precision with respect to previous CDF determinations [12].

Acknowledgements

We express our gratitude to our colleagues in the CERN accelerator departments for the excellent performance of the LHC. We thank the technical and administrative staff at the LHCb institutes. We acknowledge support from CERN and from the national agencies: CAPES, CNPq, FAPERJ and FINEP (Brazil); MOST and NSFC (China); CNRS/IN2P3 (France); BMBF, DFG and MPG (Germany); INFN (Italy); NWO (Netherlands); MNiSW and NCN (Poland); MEN/IFA (Romania); MinES and FASO (Russia); MINECO (Spain); SNSF and SER (Switzerland); NASU (Ukraine); STFC (United Kingdom); NSF (USA). We acknowledge the computing resources that are provided by CERN, IN2P3 (France), KIT and DESY (Germany), INFN (Italy), SURF (Netherlands), PIC (Spain), GridPP (United Kingdom), RRCKI and Yandex LLC (Russia), CSCS (Switzerland), IFIN-HH (Romania), CBPF (Brazil), PL-GRID (Poland) and OSC (USA). We are indebted to the communities behind the multiple open-source software packages on which we depend. Individual groups or members have received support from AvH Foundation (Germany); EPLANET, Marie Skłodowska-Curie Actions and ERC (European Union); ANR, Labex P2IO and OCEVU, and Région Auvergne-Rhône-Alpes (France); Key Research Program of Frontier Sciences of CAS, CAS PIIFL, and the Thousand Talents Program (China); RFBR, RSF and Yandex LLC (Russia); GVA, XuntaGal and GENCAT (Spain); the Royal Society and the Leverhulme Trust (United Kingdom); Laboratory Directed Research and Development program of LANL (USA).

References

- [1] N. Cabibbo, Unitary symmetry and leptonic decays, *Phys. Rev. Lett.* **10** (1963) 531.
- [2] M. Kobayashi, T. Maskawa, CP violation in the renormalizable theory of weak interaction, *Prog. Theor. Phys.* **49** (1973) 652.

- [3] J.H. Christenson, J.W. Cronin, V.L. Fitch, R. Turlay, Evidence for the 2π decay of the K_2^0 meson, Phys. Rev. Lett. 13 (1964) 138.
- [4] BaBar Collaboration, B. Aubert, et al., Observation of CP violation in the B^0 meson system, Phys. Rev. Lett. 87 (2001) 091801, arXiv:hep-ex/0107013.
- [5] Belle Collaboration, K. Abe, et al., Observation of large CP violation in the neutral B meson system, Phys. Rev. Lett. 87 (2001) 091802, arXiv:hep-ex/0107061.
- [6] BaBar Collaboration, B. Aubert, et al., Observation of direct CP violation in $B^0 \rightarrow K^+\pi^-$ decays, Phys. Rev. Lett. 93 (2004) 131801, arXiv:hep-ex/0407057.
- [7] Belle Collaboration, K. Abe, et al., Observation of large CP violation and evidence for direct CP violation in $B^0 \rightarrow \pi^+\pi^-$ decays, Phys. Rev. Lett. 93 (2004) 021601, arXiv:hep-ex/0401029.
- [8] BaBar Collaboration, B. Aubert, et al., Observation of CP violation in $B^0 \rightarrow K^+\pi^-$ and $B^0 \rightarrow \pi^+\pi^-$, Phys. Rev. Lett. 99 (2007) 021603, arXiv:hep-ex/0703016.
- [9] BaBar Collaboration, J.P. Lees, et al., Measurement of CP asymmetries and branching fractions in charmless two-body B -meson decays to pions and kaons, Phys. Rev. D 87 (2013) 052009, arXiv:1206.3525.
- [10] Belle Collaboration, J. Dalseno, et al., Measurement of the CP violation parameters in $B^0 \rightarrow \pi^+\pi^-$ decays, Phys. Rev. D 88 (2013) 092003, arXiv:1302.0551.
- [11] Belle Collaboration, Y.-T. Duh, et al., Measurements of branching fractions and direct CP asymmetries for $B \rightarrow K\pi$, $B \rightarrow \pi\pi$ and $B \rightarrow KK$ decays, Phys. Rev. D 87 (2013) 031103, arXiv:1210.1348.
- [12] CDF Collaboration, T.A. Aaltonen, et al., Measurements of direct CP-violating asymmetries in charmless decays of bottom baryons, Phys. Rev. Lett. 113 (2014) 242001, arXiv:1403.5586.
- [13] LHCb Collaboration, R. Aaij, et al., Observation of CP violation in $B^\pm \rightarrow DK^\pm$ decays, Phys. Lett. B 712 (2012) 203; R. Aaij, et al., Phys. Lett. B 713 (2012) 351 (Erratum) arXiv:1203.3662.
- [14] LHCb Collaboration, R. Aaij, et al., First observation of CP violation in the decays of B_s^0 mesons, Phys. Rev. Lett. 110 (2013) 221601, arXiv:1304.6173.
- [15] LHCb Collaboration, R. Aaij, et al., Measurement of matter–antimatter differences in beauty baryon decays, Nat. Phys. 13 (2017) 391, arXiv:1609.05216.
- [16] Y.K. Hsiao, C.Q. Geng, Direct CP violation in A_b^0 decays, Phys. Rev. D 91 (2015) 116007, arXiv:1412.1899.
- [17] A. Ali, G. Kramer, C.-D. Lü, Experimental tests of factorization in charmless nonleptonic two-body B decays, Phys. Rev. D 58 (1998) 094009, arXiv:hep-ph/9804363.
- [18] C.-D. Lü, et al., Anatomy of the perturbative QCD approach to the baryonic decays $A_b^0 \rightarrow p\pi$, pK , Phys. Rev. D 80 (2009) 034011, arXiv:0906.1479.
- [19] LHCb Collaboration, A.A. Alves Jr., et al., The LHCb detector at the LHC, J. Instrum. 3 (2008) S08005.
- [20] LHCb Collaboration, R. Aaij, et al., LHCb detector performance, Int. J. Mod. Phys. A 30 (2015) 1530022, arXiv:1412.6352.
- [21] R. Aaij, et al., Performance of the LHCb vertex locator, J. Instrum. 9 (2014) P09007, arXiv:1405.7808.
- [22] R. Arink, et al., Performance of the LHCb outer tracker, J. Instrum. 9 (2014) P01002, arXiv:1311.3893.
- [23] M. Adinolfi, et al., Performance of the LHCb RICH detector at the LHC, Eur. Phys. J. C 73 (2013) 2431, arXiv:1211.6759.
- [24] A.A. Alves Jr., et al., Performance of the LHCb muon system, J. Instrum. 8 (2013) P02022, arXiv:1211.1346.
- [25] R. Aaij, et al., The LHCb trigger and its performance in 2011, J. Instrum. 8 (2013) P04022, arXiv:1211.3055.
- [26] T. Sjöstrand, S. Mrenna, P. Skands, A brief introduction to PYTHIA 8.1, Comput. Phys. Commun. 178 (2008) 852, arXiv:0710.3820.
- [27] I. Belyaev, et al., Handling of the generation of primary events in Gauss, the LHCb simulation framework, J. Phys. Conf. Ser. 331 (2011) 032047.
- [28] D.J. Lange, The EvtGen particle decay simulation package, Nucl. Instrum. Methods Phys. Res., Sect. A 462 (2001) 152.
- [29] P. Golonka, Z. Was, PHOTOS Monte Carlo: a precision tool for QED corrections in Z and W decays, Eur. Phys. J. C 45 (2006) 97, arXiv:hep-ph/0506026.
- [30] Geant4 Collaboration, J. Allison, et al., Geant4 developments and applications, IEEE Trans. Nucl. Sci. 53 (2006) 270; Geant4 Collaboration, S. Agostinelli, et al., Geant4: a simulation toolkit, Nucl. Instrum. Methods Phys. Res., Sect. A 506 (2003) 250.
- [31] M. Clemencic, et al., The LHCb simulation application, Gauss: design, evolution and experience, J. Phys. Conf. Ser. 331 (2011) 032023.
- [32] LHCb Collaboration, R. Aaij, et al., Measurement of CP asymmetry in $D^0 \rightarrow K^-K^+$ and $D^0 \rightarrow \pi^-\pi^+$ decays, J. High Energy Phys. 07 (2014) 041, arXiv:1405.2797.
- [33] LHCb Collaboration, R. Aaij, et al., Measurement of the $D_s^+ - D_s^-$ production asymmetry in 7 TeV pp collisions, Phys. Lett. B 713 (2012) 186, arXiv:1205.0897.
- [34] LHCb Collaboration, R. Aaij, et al., Measurement of B^0, B_s^0, B^+ and Λ_b^0 production asymmetries in 7 and 8 TeV pp collisions, Phys. Lett. B 774 (2017) 139, arXiv:1703.08464.
- [35] B.P. Roe, et al., Boosted decision trees as an alternative to artificial neural networks for particle identification, Nucl. Instrum. Methods Phys. Res., Sect. A 543 (2005) 577, arXiv:physics/0408124.
- [36] L. Breiman, J.H. Friedman, R.A. Olshen, C.J. Stone, Classification and Regression Trees, Wadsworth International Group, Belmont, California, USA, 1984.
- [37] E. Baracchini, G. Isidori, Electromagnetic corrections to non-leptonic two-body B and D decays, Phys. Lett. B 633 (2006) 309, arXiv:hep-ph/0508071.
- [38] ARGUS Collaboration, H. Albrecht, et al., Measurement of the polarization in the decay $B \rightarrow J/\psi K^*$, Phys. Lett. B 340 (1994) 217.
- [39] K.S. Cranmer, Kernel estimation in high-energy physics, Comput. Phys. Commun. 136 (2001) 198, arXiv:hep-ex/0011057.
- [40] M. Pivk, F.R. Le Diberder, sPlot: a statistical tool to unfold data distributions, Nucl. Instrum. Methods Phys. Res., Sect. A 555 (2005) 356, arXiv:physics/0402083.

LHCb Collaboration

R. Aaij²⁷, B. Adeva⁴¹, M. Adinolfi⁴⁸, C.A. Aidala⁷³, Z. Ajaltouni⁵, S. Akar⁵⁹, P. Albicocco¹⁸, J. Albrecht¹⁰, F. Alessio⁴², M. Alexander⁵³, A. Alfonso Albero⁴⁰, S. Ali²⁷, G. Alkhazov³³, P. Alvarez Cartelle⁵⁵, A.A. Alves Jr⁴¹, S. Amato², S. Amerio²³, Y. Amhis⁷, L. An³, L. Anderlini¹⁷, G. Andreassi⁴³, M. Andreotti^{16,g}, J.E. Andrews⁶⁰, R.B. Appleby⁵⁶, F. Archilli²⁷, P. d'Argent¹², J. Arnau Romeu⁶, A. Artamonov³⁹, M. Artuso⁶¹, K. Arzymatov³⁷, E. Aslanides⁶, M. Atzeni⁴⁴, B. Audurier²², S. Bachmann¹², J.J. Back⁵⁰, S. Baker⁵⁵, V. Balagura^{7,b}, W. Baldini¹⁶, A. Baranov³⁷, R.J. Barlow⁵⁶, S. Barsuk⁷, W. Barter⁵⁶, F. Baryshnikov⁷⁰, V. Batozskaya³¹, B. Batsukh⁶¹, V. Battista⁴³, A. Bay⁴³, J. Beddow⁵³, F. Bedeschi²⁴, I. Bediaga¹, A. Beiter⁶¹, L.J. Bel²⁷, S. Belin²², N. Belyi⁶³, V. Bellee⁴³, N. Belloli^{20,i}, K. Belous³⁹, I. Belyaev^{34,42}, E. Ben-Haim⁸, G. Bencivenni¹⁸, S. Benson²⁷, S. Beranek⁹, A. Berezhnoy³⁵, R. Bernet⁴⁴, D. Berninghoff¹², E. Bertholet⁸, A. Bertolin²³, C. Betancourt⁴⁴, F. Betti^{15,42}, M.O. Bettler⁴⁹, M. van Beuzekom²⁷, Ia. Bezshyiko⁴⁴, S. Bhasin⁴⁸, J. Bhom²⁹, S. Bifani⁴⁷, P. Billoir⁸, A. Birnkraut¹⁰, A. Bizzeti^{17,u}, M. Bjørn⁵⁷, M.P. Blago⁴², T. Blake⁵⁰, F. Blanc⁴³, S. Blusk⁶¹, D. Bobulska⁵³, V. Bocci²⁶, O. Boente Garcia⁴¹, T. Boettcher⁵⁸, A. Bondar^{38,w}, N. Bondar³³, S. Borghi^{56,42}, M. Borisjak³⁷, M. Borsato⁴¹, F. Bossu⁷, M. Bouabdil⁹, T.J.V. Bowcock⁵⁴, C. Bozzi^{16,42}, S. Braun¹², M. Brodski⁴², J. Brodzicka²⁹, A. Brossa Gonzalo⁵⁰, D. Brundu²², E. Buchanan⁴⁸, A. Buonaura⁴⁴, C. Burr⁵⁶, A. Bursche²², J. Buytaert⁴², W. Byczynski⁴², S. Cadeddu²², H. Cai⁶⁴, R. Calabrese^{16,g}, R. Calladine⁴⁷, M. Calvi^{20,i}, M. Calvo Gomez^{40,m}, A. Camboni^{40,m}, P. Campana¹⁸, D.H. Campora Perez⁴², L. Capriotti⁵⁶, A. Carbone^{15,e}, G. Carboni²⁵, R. Cardinale^{19,h}, A. Cardini²², P. Carniti^{20,i}, L. Carson⁵², K. Carvalho Akiba², G. Casse⁵⁴, L. Cassina²⁰, M. Cattaneo⁴², G. Cavallero^{19,h}, R. Cenci^{24,p}, D. Chamont⁷,

M.G. Chapman ⁴⁸, M. Charles ⁸, Ph. Charpentier ⁴², G. Chatzikonstantinidis ⁴⁷, M. Chefdeville ⁴, V. Chekalina ³⁷, C. Chen ³, S. Chen ²², S.-G. Chitic ⁴², V. Chobanova ⁴¹, M. Chrzaszcz ⁴², A. Chubykin ³³, P. Ciambrone ¹⁸, X. Cid Vidal ⁴¹, G. Ciezarek ⁴², P.E.L. Clarke ⁵², M. Clemencic ⁴², H.V. Cliff ⁴⁹, J. Closier ⁴², V. Coco ⁴², J.A.B. Coelho ⁷, J. Cogan ⁶, E. Cogneras ⁵, L. Cojocariu ³², P. Collins ⁴², T. Colombo ⁴², A. Comerma-Montells ¹², A. Contu ²², G. Coombs ⁴², S. Coquereau ⁴⁰, G. Corti ⁴², M. Corvo ^{16,g}, C.M. Costa Sobral ⁵⁰, B. Couturier ⁴², G.A. Cowan ⁵², D.C. Craik ⁵⁸, A. Crocombe ⁵⁰, M. Cruz Torres ¹, R. Currie ⁵², C. D'Ambrosio ⁴², F. Da Cunha Marinho ², C.L. Da Silva ⁷⁴, E. Dall'Occo ²⁷, J. Dalseno ⁴⁸, A. Danilina ³⁴, A. Davis ³, O. De Aguiar Francisco ⁴², K. De Bruyn ⁴², S. De Capua ⁵⁶, M. De Cian ⁴³, J.M. De Miranda ¹, L. De Paula ², M. De Serio ^{14,d}, P. De Simone ¹⁸, C.T. Dean ⁵³, D. Decamp ⁴, L. Del Buono ⁸, B. Delaney ⁴⁹, H.-P. Dembinski ¹¹, M. Demmer ¹⁰, A. Dendek ³⁰, D. Derkach ³⁷, O. Deschamps ⁵, F. Desse ⁷, F. Dettori ⁵⁴, B. Dey ⁶⁵, A. Di Canto ⁴², P. Di Nezza ¹⁸, S. Didenko ⁷⁰, H. Dijkstra ⁴², F. Dordei ⁴², M. Dorigo ^{42,y}, A. Dosil Suárez ⁴¹, L. Douglas ⁵³, A. Dovbnya ⁴⁵, K. Dreimanis ⁵⁴, L. Dufour ²⁷, G. Dujany ⁸, P. Durante ⁴², J.M. Durham ⁷⁴, D. Dutta ⁵⁶, R. Dzhelyadin ³⁹, M. Dziewiecki ¹², A. Dziurda ²⁹, A. Dzyuba ³³, S. Easo ⁵¹, U. Egede ⁵⁵, V. Egorychev ³⁴, S. Eidelman ^{38,w}, S. Eisenhardt ⁵², U. Eitschberger ¹⁰, R. Ekelhof ¹⁰, L. Eklund ⁵³, S. Ely ⁶¹, A. Ene ³², S. Escher ⁹, S. Esen ²⁷, T. Evans ⁵⁹, A. Falabella ¹⁵, N. Farley ⁴⁷, S. Farry ⁵⁴, D. Fazzini ^{20,42,i}, L. Federici ²⁵, P. Fernandez Declara ⁴², A. Fernandez Prieto ⁴¹, F. Ferrari ^{15,*}, L. Ferreira Lopes ⁴³, F. Ferreira Rodrigues ², M. Ferro-Luzzi ⁴², S. Filippov ³⁶, R.A. Fini ¹⁴, M. Fiorini ^{16,g}, M. Firlej ³⁰, C. Fitzpatrick ⁴³, T. Fiutowski ³⁰, F. Fleuret ^{7,b}, M. Fontana ^{22,42}, F. Fontanelli ^{19,h}, R. Forty ⁴², V. Franco Lima ⁵⁴, M. Frank ⁴², C. Frei ⁴², J. Fu ^{21,q}, W. Funk ⁴², C. Färber ⁴², M. Féo Pereira Rivello Carvalho ²⁷, E. Gabriel ⁵², A. Gallas Torreira ⁴¹, D. Galli ^{15,e}, S. Gallorini ²³, S. Gambetta ⁵², Y. Gan ³, M. Gandelman ², P. Gandini ²¹, Y. Gao ³, L.M. Garcia Martin ⁷², B. Garcia Plana ⁴¹, J. García Pardiñas ⁴⁴, J. Garra Tico ⁴⁹, L. Garrido ⁴⁰, D. Gascon ⁴⁰, C. Gaspar ⁴², L. Gavardi ¹⁰, G. Gazzoni ⁵, D. Gerick ¹², E. Gersabeck ⁵⁶, M. Gersabeck ⁵⁶, T. Gershon ⁵⁰, D. Gerstel ⁶, Ph. Ghez ⁴, S. Giani ⁴³, V. Gibson ⁴⁹, O.G. Girard ⁴³, L. Giubega ³², K. Gizzdov ⁵², V.V. Gligorov ⁸, D. Golubkov ³⁴, A. Golutvin ^{55,70}, A. Gomes ^{1,a}, I.V. Gorelov ³⁵, C. Gotti ^{20,i}, E. Govorkova ²⁷, J.P. Grabowski ¹², R. Graciani Diaz ⁴⁰, L.A. Granado Cardoso ⁴², E. Graugés ⁴⁰, E. Graverini ⁴⁴, G. Graziani ¹⁷, A. Grecu ³², R. Greim ²⁷, P. Griffith ²², L. Grillo ⁵⁶, L. Gruber ⁴², B.R. Gruberg Cazon ⁵⁷, O. Grünberg ⁶⁷, C. Gu ³, E. Gushchin ³⁶, Yu. Guz ^{39,42}, T. Gys ⁴², C. Göbel ⁶², T. Hadavizadeh ⁵⁷, C. Hadjivasiliou ⁵, G. Haefeli ⁴³, C. Haen ⁴², S.C. Haines ⁴⁹, B. Hamilton ⁶⁰, X. Han ¹², T.H. Hancock ⁵⁷, S. Hansmann-Menzemer ¹², N. Harnew ⁵⁷, S.T. Harnew ⁴⁸, T. Harrison ⁵⁴, C. Hasse ⁴², M. Hatch ⁴², J. He ⁶³, M. Hecker ⁵⁵, K. Heinicke ¹⁰, A. Heister ¹⁰, K. Hennessy ⁵⁴, L. Henry ⁷², E. van Herwijnen ⁴², M. Heß ⁶⁷, A. Hicheur ², R. Hidalgo Charman ⁵⁶, D. Hill ⁵⁷, M. Hilton ⁵⁶, P.H. Hopchev ⁴³, W. Hu ⁶⁵, W. Huang ⁶³, Z.C. Huard ⁵⁹, W. Hulsbergen ²⁷, T. Humair ⁵⁵, M. Hushchyn ³⁷, D. Hutchcroft ⁵⁴, D. Hynds ²⁷, P. Ibis ¹⁰, M. Idzik ³⁰, P. Ilten ⁴⁷, K. Ivshin ³³, R. Jacobsson ⁴², J. Jalocha ⁵⁷, E. Jans ²⁷, A. Jawahery ⁶⁰, F. Jiang ³, M. John ⁵⁷, D. Johnson ⁴², C.R. Jones ⁴⁹, C. Joram ⁴², B. Jost ⁴², N. Jurik ⁵⁷, S. Kandybei ⁴⁵, M. Karacson ⁴², J.M. Kariuki ⁴⁸, S. Karodia ⁵³, N. Kazeev ³⁷, M. Kecke ¹², F. Keizer ⁴⁹, M. Kelsey ⁶¹, M. Kenzie ⁴⁹, T. Ketel ²⁸, E. Khairullin ³⁷, B. Khanji ¹², C. Khurewathanakul ⁴³, K.E. Kim ⁶¹, T. Kirn ⁹, S. Klaver ¹⁸, K. Klimaszewski ³¹, T. Klimkovich ¹¹, S. Koliiev ⁴⁶, M. Kolpin ¹², R. Kopecna ¹², P. Koppenburg ²⁷, I. Kostiuk ²⁷, S. Kotriakhova ³³, M. Kozeiha ⁵, L. Kravchuk ³⁶, M. Kreps ⁵⁰, F. Kress ⁵⁵, P. Krokovny ^{38,w}, W. Krupa ³⁰, W. Krzemien ³¹, W. Kucewicz ^{29,l}, M. Kucharczyk ²⁹, V. Kudryavtsev ^{38,w}, A.K. Kuonen ⁴³, T. Kvaratskheliya ^{34,42}, D. Lacarrere ⁴², G. Lafferty ⁵⁶, A. Lai ²², D. Lancierini ⁴⁴, G. Lanfranchi ¹⁸, C. Langenbruch ⁹, T. Latham ⁵⁰, C. Lazzeroni ⁴⁷, R. Le Gac ⁶, A. Leflat ³⁵, J. Lefrançois ⁷, R. Lefèvre ⁵, F. Lemaitre ⁴², O. Leroy ⁶, T. Lesiak ²⁹, B. Leverington ¹², P.-R. Li ⁶³, T. Li ³, Z. Li ⁶¹, X. Liang ⁶¹, T. Likhomanenko ⁶⁹, R. Lindner ⁴², F. Lionetto ⁴⁴, V. Lisovskyi ⁷, X. Liu ³, D. Loh ⁵⁰, A. Loi ²², I. Longstaff ⁵³, J.H. Lopes ², G.H. Lovell ⁴⁹, D. Lucchesi ^{23,o}, M. Lucio Martinez ⁴¹, A. Lupato ²³, E. Luppi ^{16,g}, O. Lupton ⁴², A. Lusiani ²⁴, X. Lyu ⁶³, F. Machefert ⁷, F. Maciuc ³², V. Macko ⁴³, P. Mackowiak ¹⁰, S. Maddrell-Mander ⁴⁸, O. Maev ^{33,42}, K. Maguire ⁵⁶, D. Maisuzenko ³³, M.W. Majewski ³⁰, S. Malde ⁵⁷, B. Malecki ²⁹, A. Malinin ⁶⁹, T. Maltsev ^{38,w}, G. Manca ^{22,f}, G. Mancinelli ⁶, D. Marangotto ^{21,q}, J. Maratas ^{5,v}, J.F. Marchand ⁴, U. Marconi ¹⁵, C. Marin Benito ⁷, M. Marinangeli ⁴³, P. Marino ⁴³, J. Marks ¹², P.J. Marshall ⁵⁴, G. Martellotti ²⁶, M. Martin ⁶, M. Martinelli ⁴², D. Martinez Santos ⁴¹, F. Martinez Vidal ⁷², A. Massafferri ¹, M. Materok ⁹, R. Matev ⁴², A. Mathad ⁵⁰, Z. Mathe ⁴², C. Matteuzzi ²⁰, A. Mauri ⁴⁴, E. Maurice ^{7,b}, B. Maurin ⁴³, A. Mazurov ⁴⁷, M. McCann ^{55,42}, A. McNab ⁵⁶, R. McNulty ¹³, J.V. Mead ⁵⁴, B. Meadows ⁵⁹,

- C. Meaux ⁶, F. Meier ¹⁰, N. Meinert ⁶⁷, D. Melnychuk ³¹, M. Merk ²⁷, A. Merli ^{21,q}, E. Michielin ²³,
 D.A. Milanes ⁶⁶, E. Millard ⁵⁰, M.-N. Minard ⁴, L. Minzoni ^{16,g}, D.S. Mitzel ¹², A. Mogini ⁸,
 J. Molina Rodriguez ^{1,z}, T. Mombächer ¹⁰, I.A. Monroy ⁶⁶, S. Monteil ⁵, M. Morandin ²³, G. Morello ¹⁸,
 M.J. Morello ^{24,t}, O. Morgunova ⁶⁹, J. Moron ³⁰, A.B. Morris ⁶, R. Mountain ⁶¹, F. Muheim ⁵², M. Mulder ²⁷,
 C.H. Murphy ⁵⁷, D. Murray ⁵⁶, A. Mödden ¹⁰, D. Müller ⁴², J. Müller ¹⁰, K. Müller ⁴⁴, V. Müller ¹⁰, P. Naik ⁴⁸,
 T. Nakada ⁴³, R. Nandakumar ⁵¹, A. Nandi ⁵⁷, T. Nanut ⁴³, I. Nasteva ², M. Needham ⁵², N. Neri ²¹,
 S. Neubert ¹², N. Neufeld ⁴², M. Neuner ¹², T.D. Nguyen ⁴³, C. Nguyen-Mau ^{43,n}, S. Nieswand ⁹, R. Niet ¹⁰,
 N. Nikitin ³⁵, A. Nogay ⁶⁹, N.S. Nolte ⁴², D.P. O'Hanlon ¹⁵, A. Oblakowska-Mucha ³⁰, V. Obraztsov ³⁹,
 S. Ogilvy ¹⁸, R. Oldeman ^{22,f}, C.J.G. Onderwater ⁶⁸, A. Ossowska ²⁹, J.M. Otalora Goicochea ², P. Owen ⁴⁴,
 A. Oyanguren ⁷², P.R. Pais ⁴³, T. Pajero ^{24,t}, A. Palano ¹⁴, M. Palutan ^{18,42}, G. Panshin ⁷¹, A. Papanestis ⁵¹,
 M. Pappagallo ⁵², L.L. Pappalardo ^{16,g}, W. Parker ⁶⁰, C. Parkes ⁵⁶, G. Passaleva ^{17,42}, A. Pastore ¹⁴,
 M. Patel ⁵⁵, C. Patrignani ^{15,e}, A. Pearce ⁴², A. Pellegrino ²⁷, G. Penso ²⁶, M. Pepe Altarelli ⁴², S. Perazzini ⁴²,
 D. Pereima ³⁴, P. Perret ⁵, L. Pescatore ⁴³, K. Petridis ⁴⁸, A. Petrolini ^{19,h}, A. Petrov ⁶⁹, S. Petrucci ⁵²,
 M. Petruzzo ^{21,q}, B. Pietrzyk ⁴, G. Pietrzyk ⁴³, M. Pikies ²⁹, M. Pili ⁵⁷, D. Pinci ²⁶, J. Pinzino ⁴², F. Pisani ⁴²,
 A. Piucci ¹², V. Placinta ³², S. Playfer ⁵², J. Plews ⁴⁷, M. Plo Casasus ⁴¹, F. Polci ⁸, M. Poli Lener ¹⁸,
 A. Poluektov ⁵⁰, N. Polukhina ^{70,c}, I. Polyakov ⁶¹, E. Polycarpo ², G.J. Pomery ⁴⁸, S. Ponce ⁴², A. Popov ³⁹,
 D. Popov ^{47,11}, S. Poslavskii ³⁹, C. Potterat ², E. Price ⁴⁸, J. Prisciandaro ⁴¹, C. Prouve ⁴⁸, V. Pugatch ⁴⁶,
 A. Puig Navarro ⁴⁴, H. Pullen ⁵⁷, G. Punzi ^{24,p}, W. Qian ⁶³, J. Qin ⁶³, R. Quagliani ⁸, B. Quintana ⁵,
 B. Rachwal ³⁰, J.H. Rademacker ⁴⁸, M. Rama ²⁴, M. Ramos Pernas ⁴¹, M.S. Rangel ², F. Ratnikov ^{37,x},
 G. Raven ²⁸, M. Ravonel Salzgeber ⁴², M. Reboud ⁴, F. Redi ⁴³, S. Reichert ¹⁰, A.C. dos Reis ¹, F. Reiss ⁸,
 C. Remon Alepuz ⁷², Z. Ren ³, V. Renaudin ⁷, S. Ricciardi ⁵¹, S. Richards ⁴⁸, K. Rinnert ⁵⁴, P. Robbe ⁷,
 A. Robert ⁸, A.B. Rodrigues ⁴³, E. Rodrigues ⁵⁹, J.A. Rodriguez Lopez ⁶⁶, M. Roehrken ⁴², A. Rogozhnikov ³⁷,
 S. Roiser ⁴², A. Rollings ⁵⁷, V. Romanovskiy ³⁹, A. Romero Vidal ⁴¹, M. Rotondo ¹⁸, M.S. Rudolph ⁶¹,
 T. Ruf ⁴², J. Ruiz Vidal ⁷², J.J. Saborido Silva ⁴¹, N. Sagidova ³³, B. Saitta ^{22,f}, V. Salustino Guimaraes ⁶²,
 C. Sanchez Gras ²⁷, C. Sanchez Mayordomo ⁷², B. Sanmartin Sedes ⁴¹, R. Santacesaria ²⁶,
 C. Santamarina Rios ⁴¹, M. Santimaria ¹⁸, E. Santovetti ^{25,j}, G. Sarpis ⁵⁶, A. Sarti ^{18,k}, C. Satriano ^{26,s},
 A. Satta ²⁵, M. Saur ⁶³, D. Savrina ^{34,35}, S. Schael ⁹, M. Schellenberg ¹⁰, M. Schiller ⁵³, H. Schindler ⁴²,
 M. Schmelling ¹¹, T. Schmelzer ¹⁰, B. Schmidt ⁴², O. Schneider ⁴³, A. Schopper ⁴², H.F. Schreiner ⁵⁹,
 M. Schubiger ⁴³, M.H. Schune ⁷, R. Schwemmer ⁴², B. Sciascia ¹⁸, A. Sciubba ^{26,k}, A. Semennikov ³⁴,
 E.S. Sepulveda ⁸, A. Sergi ^{47,42}, N. Serra ⁴⁴, J. Serrano ⁶, L. Sestini ²³, A. Seuthe ¹⁰, P. Seyfert ⁴²,
 M. Shapkin ³⁹, Y. Shcheglov ^{33,†}, T. Shears ⁵⁴, L. Shekhtman ^{38,w}, V. Shevchenko ⁶⁹, E. Shmanin ⁷⁰,
 B.G. Siddi ¹⁶, R. Silva Coutinho ⁴⁴, L. Silva de Oliveira ², G. Simi ^{23,o}, S. Simone ^{14,d}, N. Skidmore ¹²,
 T. Skwarnicki ⁶¹, J.G. Smeaton ⁴⁹, E. Smith ⁹, I.T. Smith ⁵², M. Smith ⁵⁵, M. Soares ¹⁵, I. Soares Lavra ¹,
 M.D. Sokoloff ⁵⁹, F.J.P. Soler ⁵³, B. Souza De Paula ², B. Spaan ¹⁰, P. Spradlin ⁵³, F. Stagni ⁴², M. Stahl ¹²,
 S. Stahl ⁴², P. Steffko ⁴³, S. Stefkova ⁵⁵, O. Steinkamp ⁴⁴, S. Stemmle ¹², O. Stenyakin ³⁹, M. Stepanova ³³,
 H. Stevens ¹⁰, A. Stocchi ⁷, S. Stone ⁶¹, B. Storaci ⁴⁴, S. Stracka ^{24,p}, M.E. Stramaglia ⁴³, M. Straticiuc ³²,
 U. Straumann ⁴⁴, S. Strokov ⁷¹, J. Sun ³, L. Sun ⁶⁴, K. Swientek ³⁰, V. Syropoulos ²⁸, T. Szumlak ³⁰,
 M. Szymanski ⁶³, S. T'Jampens ⁴, Z. Tang ³, A. Tayduganov ⁶, T. Tekampe ¹⁰, G. Tellarini ¹⁶, F. Teubert ⁴²,
 E. Thomas ⁴², J. van Tilburg ²⁷, M.J. Tilley ⁵⁵, V. Tisserand ⁵, M. Tobin ³⁰, S. Tolk ⁴², L. Tomassetti ^{16,g},
 D. Tonelli ²⁴, D.Y. Tou ⁸, R. Tourinho Jadallah Aoude ¹, E. Tournefier ⁴, M. Traill ⁵³, M.T. Tran ⁴³,
 A. Trisovic ⁴⁹, A. Tsaregorodtsev ⁶, G. Tuci ²⁴, A. Tully ⁴⁹, N. Tuning ^{27,42}, A. Ukleja ³¹, A. Usachov ⁷,
 A. Ustyuzhanin ³⁷, U. Uwer ¹², A. Vagner ⁷¹, V. Vagnoni ¹⁵, A. Valassi ⁴², S. Valat ⁴², G. Valenti ¹⁵,
 R. Vazquez Gomez ⁴², P. Vazquez Regueiro ⁴¹, S. Vecchi ¹⁶, M. van Veghel ²⁷, J.J. Velthuis ⁴⁸, M. Veltri ^{17,r},
 G. Veneziano ⁵⁷, A. Venkateswaran ⁶¹, T.A. Verlage ⁹, M. Vernet ⁵, M. Veronesi ²⁷, N.V. Veronika ¹³,
 M. Vesterinen ⁵⁷, J.V. Viana Barbosa ⁴², D. Vieira ⁶³, M. Vieites Diaz ⁴¹, H. Viemann ⁶⁷,
 X. Vilasis-Cardona ^{40,m}, A. Vitkovskiy ²⁷, M. Vitti ⁴⁹, V. Volkov ³⁵, A. Vollhardt ⁴⁴, B. Voneki ⁴²,
 A. Vorobyev ³³, V. Vorobyev ^{38,w}, J.A. de Vries ²⁷, C. Vázquez Sierra ²⁷, R. Waldi ⁶⁷, J. Walsh ²⁴, J. Wang ⁶¹,
 M. Wang ³, Y. Wang ⁶⁵, Z. Wang ⁴⁴, D.R. Ward ⁴⁹, H.M. Wark ⁵⁴, N.K. Watson ⁴⁷, D. Websdale ⁵⁵,
 A. Weiden ⁴⁴, C. Weisser ⁵⁸, M. Whitehead ⁹, J. Wicht ⁵⁰, G. Wilkinson ⁵⁷, M. Wilkinson ⁶¹, I. Williams ⁴⁹,
 M.R.J. Williams ⁵⁶, M. Williams ⁵⁸, T. Williams ⁴⁷, F.F. Wilson ^{51,42}, J. Wimberley ⁶⁰, M. Winn ⁷,
 J. Wishahi ¹⁰, W. Wislicki ³¹, M. Witek ²⁹, G. Wormser ⁷, S.A. Wotton ⁴⁹, K. Wyllie ⁴², D. Xiao ⁶⁵, Y. Xie ⁶⁵,
 A. Xu ³, M. Xu ⁶⁵, Q. Xu ⁶³, Z. Xu ³, Z. Xu ⁴, Z. Yang ³, Z. Yang ⁶⁰, Y. Yao ⁶¹, L.E. Yeomans ⁵⁴, H. Yin ⁶⁵,

J. Yu^{65,ab}, X. Yuan⁶¹, O. Yushchenko³⁹, K.A. Zarebski⁴⁷, M. Zavertyaev^{11,c}, D. Zhang⁶⁵, L. Zhang³, W.C. Zhang^{3,aa}, Y. Zhang⁷, A. Zhelezov¹², Y. Zheng⁶³, X. Zhu³, V. Zhukov^{9,35}, J.B. Zonneveld⁵², S. Zucchelli¹⁵

¹ Centro Brasileiro de Pesquisas Físicas (CBPF), Rio de Janeiro, Brazil

² Universidade Federal do Rio de Janeiro (UFRJ), Rio de Janeiro, Brazil

³ Center for High Energy Physics, Tsinghua University, Beijing, China

⁴ Univ. Grenoble Alpes, Univ. Savoie Mont Blanc, CNRS, IN2P3-LAPP, Annecy, France

⁵ Clermont Université, Université Blaise Pascal, CNRS/IN2P3, LPC, Clermont-Ferrand, France

⁶ Aix Marseille Univ, CNRS/IN2P3, CPPM, Marseille, France

⁷ LAL, Univ. Paris-Sud, CNRS/IN2P3, Université Paris-Saclay, Orsay, France

⁸ LPNHE, Sorbonne Université, Paris Diderot Sorbonne Paris Cité, CNRS/IN2P3, Paris, France

⁹ I. Physikalisches Institut, RWTH Aachen University, Aachen, Germany

¹⁰ Fakultät Physik, Technische Universität Dortmund, Dortmund, Germany

¹¹ Max-Planck-Institut für Kernphysik (MPIK), Heidelberg, Germany

¹² Physikalisches Institut, Ruprecht-Karls-Universität Heidelberg, Heidelberg, Germany

¹³ School of Physics, University College Dublin, Dublin, Ireland

¹⁴ INFN Sezione di Bari, Bari, Italy

¹⁵ INFN Sezione di Bologna, Bologna, Italy

¹⁶ INFN Sezione di Ferrara, Ferrara, Italy

¹⁷ INFN Sezione di Firenze, Firenze, Italy

¹⁸ INFN Laboratori Nazionali di Frascati, Frascati, Italy

¹⁹ INFN Sezione di Genova, Genoa, Italy

²⁰ INFN Sezione di Milano-Bicocca, Milano, Italy

²¹ INFN Sezione di Milano, Milano, Italy

²² INFN Sezione di Cagliari, Monserrato, Italy

²³ INFN Sezione di Padova, Padova, Italy

²⁴ INFN Sezione di Pisa, Pisa, Italy

²⁵ INFN Sezione di Roma Tor Vergata, Roma, Italy

²⁶ INFN Sezione di Roma La Sapienza, Roma, Italy

²⁷ Nikhef National Institute for Subatomic Physics, Amsterdam, Netherlands

²⁸ Nikhef National Institute for Subatomic Physics and VU University Amsterdam, Amsterdam, Netherlands

²⁹ Henryk Niewodniczanski Institute of Nuclear Physics Polish Academy of Sciences, Kraków, Poland

³⁰ AGH – University of Science and Technology, Faculty of Physics and Applied Computer Science, Kraków, Poland

³¹ National Center for Nuclear Research (NCBJ), Warsaw, Poland

³² Horia Hulubei National Institute of Physics and Nuclear Engineering, Bucharest-Magurele, Romania

³³ Petersburg Nuclear Physics Institute (PNPI), Gatchina, Russia

³⁴ Institute of Theoretical and Experimental Physics (ITEP), Moscow, Russia

³⁵ Institute of Nuclear Physics, Moscow State University (SINP MSU), Moscow, Russia

³⁶ Institute for Nuclear Research of the Russian Academy of Sciences (INR RAS), Moscow, Russia

³⁷ Yandex School of Data Analysis, Moscow, Russia

³⁸ Budker Institute of Nuclear Physics (SB RAS), Novosibirsk, Russia

³⁹ Institute for High Energy Physics (IHEP), Protvino, Russia

⁴⁰ ICCUB, Universitat de Barcelona, Barcelona, Spain

⁴¹ Instituto Galego de Física de Altas Energías (IGFAE), Universidade de Santiago de Compostela, Santiago de Compostela, Spain

⁴² European Organization for Nuclear Research (CERN), Geneva, Switzerland

⁴³ Institute of Physics, Ecole Polytechnique Fédérale de Lausanne (EPFL), Lausanne, Switzerland

⁴⁴ Physik-Institut, Universität Zürich, Zürich, Switzerland

⁴⁵ NSC Kharkiv Institute of Physics and Technology (NSC KIPT), Kharkiv, Ukraine

⁴⁶ Institute for Nuclear Research of the National Academy of Sciences (KINR), Kyiv, Ukraine

⁴⁷ University of Birmingham, Birmingham, United Kingdom

⁴⁸ H.H. Wills Physics Laboratory, University of Bristol, Bristol, United Kingdom

⁴⁹ Cavendish Laboratory, University of Cambridge, Cambridge, United Kingdom

⁵⁰ Department of Physics, University of Warwick, Coventry, United Kingdom

⁵¹ STFC Rutherford Appleton Laboratory, Didcot, United Kingdom

⁵² School of Physics and Astronomy, University of Edinburgh, Edinburgh, United Kingdom

⁵³ School of Physics and Astronomy, University of Glasgow, Glasgow, United Kingdom

⁵⁴ Oliver Lodge Laboratory, University of Liverpool, Liverpool, United Kingdom

⁵⁵ Imperial College London, London, United Kingdom

⁵⁶ School of Physics and Astronomy, University of Manchester, Manchester, United Kingdom

⁵⁷ Department of Physics, University of Oxford, Oxford, United Kingdom

⁵⁸ Massachusetts Institute of Technology, Cambridge, MA, United States

⁵⁹ University of Cincinnati, Cincinnati, OH, United States

⁶⁰ University of Maryland, College Park, MD, United States

⁶¹ Syracuse University, Syracuse, NY, United States

⁶² Pontifícia Universidade Católica do Rio de Janeiro (PUC-Rio), Rio de Janeiro, Brazil ^{ac}

⁶³ University of Chinese Academy of Sciences, Beijing, China ^{ad}

⁶⁴ School of Physics and Technology, Wuhan University, Wuhan, China ^{ad}

⁶⁵ Institute of Particle Physics, Central China Normal University, Wuhan, Hubei, China ^{ad}

⁶⁶ Departamento de Física, Universidad Nacional de Colombia, Bogota, Colombia ^{ae}

⁶⁷ Institut für Physik, Universität Rostock, Rostock, Germany ^{af}

⁶⁸ Van Swinderen Institute, University of Groningen, Groningen, Netherlands ^{ag}

⁶⁹ National Research Centre Kurchatov Institute, Moscow, Russia ^{ah}

⁷⁰ National University of Science and Technology "MISIS", Moscow, Russia ^{ah}

⁷¹ National Research Tomsk Polytechnic University, Tomsk, Russia ^{ai}

⁷² Instituto de Física Corpuscular, Centro Mixto Universidad de Valencia – CSIC, Valencia, Spain ^{ai}

⁷³ University of Michigan, Ann Arbor, United States ^{aj}

⁷⁴ Los Alamos National Laboratory (LANL), Los Alamos, United States ^{aj}

- * Corresponding author.
E-mail address: fabio.ferrari@cern.ch (F. Ferrari).
- ^a Universidade Federal do Triângulo Mineiro (UFTM), Uberaba-MG, Brazil.
- ^b Laboratoire Leprince-Ringuet, Palaiseau, France.
- ^c P.N. Lebedev Physical Institute, Russian Academy of Science (LPI RAS), Moscow, Russia.
- ^d Università di Bari, Bari, Italy.
- ^e Università di Bologna, Bologna, Italy.
- ^f Università di Cagliari, Cagliari, Italy.
- ^g Università di Ferrara, Ferrara, Italy.
- ^h Università di Genova, Genova, Italy.
- ⁱ Università di Milano Bicocca, Milano, Italy.
- ^j Università di Roma Tor Vergata, Roma, Italy.
- ^k Università di Roma La Sapienza, Roma, Italy.
- ^l AGH – University of Science and Technology, Faculty of Computer Science, Electronics and Telecommunications, Kraków, Poland.
- ^m LIFAELS, La Salle, Universitat Ramon Llull, Barcelona, Spain.
- ⁿ Hanoi University of Science, Hanoi, Vietnam.
- ^o Università di Padova, Padova, Italy.
- ^p Università di Pisa, Pisa, Italy.
- ^q Università degli Studi di Milano, Milano, Italy.
- ^r Università di Urbino, Urbino, Italy.
- ^s Università della Basilicata, Potenza, Italy.
- ^t Scuola Normale Superiore, Pisa, Italy.
- ^u Università di Modena e Reggio Emilia, Modena, Italy.
- ^v MSU – Iligan Institute of Technology (MSU-IIT), Iligan, Philippines.
- ^w Novosibirsk State University, Novosibirsk, Russia.
- ^x National Research University Higher School of Economics, Moscow, Russia.
- ^y Sezione INFN di Trieste, Trieste, Italy.
- ^z Escuela Agrícola Panamericana, San Antonio de Oriente, Honduras.
- ^{aa} School of Physics and Information Technology, Shaanxi Normal University (SNNU), Xi'an, China.
- ^{ab} Physics and Micro Electronic College, Hunan University, Changsha City, China.
- ^{ac} Associated to Universidade Federal do Rio de Janeiro (UFRJ), Rio de Janeiro, Brazil.
- ^{ad} Associated to Center for High Energy Physics, Tsinghua University, Beijing, China.
- ^{ae} Associated to LPNHE, Sorbonne Université, Paris Diderot Sorbonne Paris Cité, CNRS/IN2P3, Paris, France.
- ^{af} Associated to Physikalisches Institut, Ruprecht-Karls-Universität Heidelberg, Heidelberg, Germany.
- ^{ag} Associated to Nikhef National Institute for Subatomic Physics, Amsterdam, Netherlands.
- ^{ah} Associated to Institute of Theoretical and Experimental Physics (ITEP), Moscow, Russia.
- ^{ai} Associated to ICCUB, Universitat de Barcelona, Barcelona, Spain.
- ^{aj} Associated to Syracuse University, Syracuse, NY, United States.
- † Deceased.